SEIR epidemic model for COVID-19 transmission by Caputo derivative of fractional order

Shahram Rezapour[1,2,3], Hakimeh Mohammadi[4*] and Mohammad Esmael Samei[5]

*Correspondence:
hakimeh.mohammadi@yahoo.com
[4]Department of Mathematics,
Miandoab Branch, Islamic Azad
University, Miandoab, Iran
Full list of author information is
available at the end of the article

Abstract

We provide a SEIR epidemic model for the spread of COVID-19 using the Caputo fractional derivative. The feasibility region of the system and equilibrium points are calculated and the stability of the equilibrium points is investigated. We prove the existence of a unique solution for the model by using fixed point theory. Using the fractional Euler method, we get an approximate solution to the model. To predict the transmission of COVID-19 in Iran and in the world, we provide a numerical simulation based on real data.

MSC: Primary 34A08; secondary 65P99; 49J15

Keywords: COVID-19; Equilibrium point; Numerical simulation; SEIR model

1 Introduction

Coronaviruses are crown viruses that can cause disease in humans and animals. In humans, several coronaviruses are known to cause respiratory illnesses such as common cold and more severe illnesses such as acute Middle East respiratory syndrome (SARS), severe acute respiratory syndrome (SARS), and a recently discovered disease COVID-19. A coronavirus (COVID-19) that was first identified in the Chinese city of Wuhan in 2019 is a new strain that has not been previously identified in humans. Snakes or bats have been suspected as a potential source for the outbreak, though other experts currently consider this to be unlikely. Fever, cough, shortness of breath, and breathing difficulties are initial symptoms of this infection. In the next steps, the infection can cause pneumonia, severe acute respiratory syndrome, kidney failure, and even death.

The study of disease dynamics is a dominating theme for many biologists and mathematicians (see, for example, [1–12]). In recent years, many physical and biological problems have been modeled by fractional-order derivatives. The main reasons for using a fractional-order system (FDE) is related to systems with memory, history, or nonlocal effects which exist in many biological systems that show the realistic biphasic decline behavior of infection or diseases but at a slower rate. It has been studied by many researchers that fractional extensions of mathematical models of integer order represent the natural fact in a very systematic way such as in the approach of Etemad et al. [13–15], Hedayati

et al. [13, 16–19], Baleanu et al. [11, 18, 20, 21], and Mahdy et al. [22, 23]. In recent years, many papers have been published on the subject of Caputo–Fabrizio fractional derivative (see, for example, [24–30]). Mathematical models are used to simulate the transmission of coronavirus (see, for example, [31–37]).

In this paper, we intend to investigate the spread of COVID-19 disease using the SEIR mathematical model with the Caputo fractional-order derivative. First, we analyze the model mathematically and then, in the numerical section, we present simulations for the release of COVID-19 in Iran and around the world. Also, to evaluate the advantage of using the fraction derivative, we make a comparison between the results of the model with the fractional- and integer-order derivative with the real data to determine which one provides a better approximation in this model. By calculating the model results for different orders of fractional derivative, we investigate the effect of derivative order on the behavior of the resulting functions and equilibrium points and resulting numerical values.

The structure of the paper is as follows. In Sect. 2 some basic definitions and concepts of fractional calculus are recalled. The SEIR model of fractional order for COVID-19 transmission is presented in Sect. 3, and the equilibrium points and the reproduction number are calculated. The stability of the equilibrium points is analyzed in Sect. 4. The existence and uniqueness of solution for the system is proved in Sect. 5. In Sect. 6, a numerical method for solving the model is described and a numerical simulation is presented.

2 Preliminary results and definitions

In this section, we recall some of the fundamental concepts of fractional differential calculus, which are found in many books and papers.

Definition 1 ([38]) For an integrable function g, the Caputo derivative of fractional order $v \in (0, 1)$ is given by

$$^{C}D^{v}g(t) = \frac{1}{\Gamma(m - v)} \int_{0}^{t} \frac{g^{(m)}(v)}{(t - v)^{v - m + 1}} \, dv, \quad m = [v] + 1.$$

Also, the corresponding fractional integral of order v with $Re(v) > 0$ is given by

$$^{C}I^{v}g(t) = \frac{1}{\Gamma(v)} \int_{0}^{t} (t - v)^{v - 1} g(v) \, dv.$$

Definition 2 ([24, 39]) For $g \in H^{1}(c, d)$ and $d > c$, the Caputo–Fabrizio derivative of fractional order $v \in (0, 1)$ for g is given by

$$^{CF}D^{v}g(t) = \frac{M(v)}{(1 - v)} \int_{c}^{t} exp\left(\frac{-v}{1 - v}(t - v)\right) g'(v) \, dv,$$

where $t \geq 0$, $M(v)$ is a normalization function that depends on v and $M(0) = M(1) = 1$. If $g \notin H^{1}(c, d)$ and $0 < v < 1$, this derivative for $g \in L^{1}(-\infty, d)$ is given by

$$^{CF}D^{v}g(t) = \frac{vM(v)}{(1 - v)} \int_{-\infty}^{d} (g(t) - g(v)) exp\left(\frac{-v}{1 - v}(t - v)\right) dv.$$

Also, the corresponding *CF* fractional integral is presented by

$$
{}^{CF}I^\nu g(t) = \frac{2(1-\nu)}{(2-\nu)M(\nu)}g(t) + \frac{2\nu}{(2-\nu)M(\nu)} \int_0^t g(\upsilon)\,d\upsilon.
$$

Definition 3 ([40]) Let $b > a$, $g \in H^1(a,b)$, and $0 < \nu < 1$, then the fractional Atangana–Baleanu derivative in the Caputo sense is defined by

$$
{}^{ABC}D^\nu g(t) = \frac{B(\nu)}{(1-\nu)} \int_a^t g'(s)E_\nu\left(\frac{-\nu}{1-\nu}(t-\upsilon)^\nu\right)d\upsilon,
$$

where $B(\nu)$ denotes the normalization function satisfying $B(0) = B(1) = 1$ and $E_\nu(\cdot)$ is a one-parameter Mittag-Leffler function. Also, the Atangana–Baleanu fractional integral is given as follows:

$$
{}^{ABC}I^\nu g(t) = \frac{1-\nu}{B(\nu)}g(t) + \frac{\nu}{B(\nu)\Gamma(\nu)} \int_a^t g(\upsilon)(t-\upsilon)^{\nu-1}\,d\upsilon.
$$

The Laplace transform is one of the important tools in solving differential equations that are defined below for two kinds of fractional derivative.

Definition 4 ([38]) The Laplace transform of the Caputo fractional differential operator of order ν is given by

$$
L\big[{}^C D^\nu g(t)\big](s) = s^\nu Lg(t) - \sum_{i=0}^{m-1} s^{\nu-i-1}g^{(i)}(0), \quad m-1 < \nu \le m \in N,
$$

which can also be obtained in the form

$$
L\big[{}^C D^\nu g(t)\big] = \frac{s^m L[g(t)] - s^{m-1}g(0) - s^{m-1}g'(0) - \cdots - g^{(m-1)}}{s^{m-\nu}}.
$$

3 Model formulation

In viral epidemic diseases, mathematical models are very important for predicting the transmission of the virus by considering its behavior in different regions for helping to manage the disease. Different mathematical models such as SIR, SEIR, SIRD, SEIRD, SIRS, SIRC, MSEIR, SEAIHRD, etc. are used to investigate the spread of diseases. According to the information published about COVID-19 by the World Health Organization, there are two types of people with the disease: one group has no symptoms and the other group has symptoms. Both groups transmit the disease to healthy people, and the sick people either recover or die. Of course, during this process, more groups can be considered, such as people who are hospitalized, but because we do not have accurate information about these groups for simulation, we decided to use the simple SEIR model. In this model, we divide people into four groups: susceptible people (S), exposed or asymptomatic infected people (E), symptomatic infected people (I), and recovered people (R) including improved people. The diagram for the dynamics of COVID-19 disease model is shown in Fig. 1.

Figure 1 The diagram for the proposed model of COVID-19
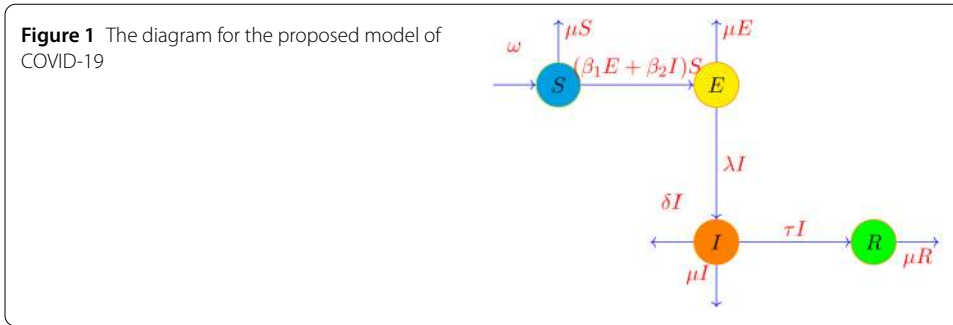
Based on Fig. 1, we consider the SEIR model for COVID-19 as follows:

$$
\begin{cases}
\frac{dS}{dt} = \omega - (\beta_1 E + \beta_2 I)S - \mu S, \\
\frac{dE}{dt} = (\beta_1 E + \beta_2 I)S - (\lambda + \mu)E, \\
\frac{dI}{dt} = \lambda E - (\tau + \mu + \delta)I, \\
\frac{dR}{dt} = \tau I - \mu R,
\end{cases}
$$

where

$\omega = n \times N$, N is the total number of individuals and n is the birth rate

μ: the death rate of people,

β_1: the transmission rate of infection from E to S,

β_2: the transmission rate of infection from I to S,

λ: the transmission rate of people from E to I,

δ: the mortality rate due to the disease,

τ: the rate of recovery of infected people,

with the initial conditions $S(0) = S_0 > 0$, $E(0) = E_0 > 0$, $I(0) = I_0 > 0$, $R(0) = R_0 \geq 0$.

In this section, we moderate the system by substituting the time derivative with the Caputo fractional derivative. The ordinary derivative has an inverse second dimension s^{-1} and the fractional derivative D^ν has a dimension of $s^{-\nu}$. To solve this problem, we use an auxiliary parameter θ that has a second dimension s and is called the cosmic time [41]. By the parameter, from a physical point of view, we will have $[\theta^{\nu-1}{}^C D^\nu] = [\frac{d}{dt}] = s^{-1}$.

According to the explanation presented, the COVID-19 fractional model for $t > 0$ and $\nu \in (0, 1)$ is given as follows:

$$
\begin{cases}
\theta^{\nu-1}{}^C D_t^\nu S(t) = \omega - (\beta_1 E(t) + \beta_2 I(t))S(t) - \mu S(t), \\
\theta^{\nu-1}{}^C D_t^\nu E(t) = (\beta_1 E(t) + \beta_2 I(t))S(t) - (\lambda + \mu)E(t), \\
\theta^{\nu-1}{}^C D_t^\nu I(t) = \lambda E(t) - (\tau + \mu + \delta)I(t), \\
\theta^{\nu-1}{}^C D_t^\nu R(t) = \tau I(t) - \mu R(t),
\end{cases}
\tag{1}
$$

where the initial conditions are $S(0) = S_0 > 0$, $E(0) = E_0 > 0$, $I(0) = I_0 > 0$, $R(0) = R_0 \geq 0$.

3.1 Nonnegative solution

Consider $\Upsilon = \{(S, E, I, R) \in R_4^+ : S + E + I + R \leq \frac{\omega}{\mu}\}$, we show that the closed set Υ is the feasibility region of system (1).

Lemma 5 *The closed set Υ is positively invariant with respect to fractional system* (1).

Proof To obtain the fractional derivative of total population, we add all the relations in system (1). So

$$\theta^{v-1}{}^{C}D_t^v N(t) = \omega - \mu N(t) - \delta I(t)$$
$$\leq \omega - \mu N(t),$$

where $N(t) = S(t) + E(t) + I(t) + R(t)$. Using the Laplace transform and Theorem 7.2 (and Remark 7.1) in [42], we obtain

$$N(t) \leq N(0)E_v\left(-\mu\theta^{1-v}t^v\right) + \int_0^t \omega\theta^{1-v}\eta^{v-1}E_{v,v}\left(-\mu\theta^{1-v}\eta^v\right)d\eta,$$

where $N(0)$ is the initial population size. With some calculations, we get

$$N(t) \leq N(0)E_v\left(-\mu\theta^{1-v}t^v\right) + \int_0^t \omega\theta^{1-v}\eta^{v-1}\sum_{i=0}^{\infty}\frac{(-1)^i\mu^i\theta^{i(1-v)}\eta^{iv}}{\Gamma(iv+v)}\,d\eta$$
$$= \frac{\omega\theta^{1-v}}{\mu\theta^{1-v}} + E_v\left(-\mu\theta^{1-v}t^v\right)\left(N(0) - \frac{\omega\theta^{1-v}}{\mu\theta^{1-v}}\right)$$
$$= \frac{\omega}{\mu} + E_v\left(-\mu\theta^{1-v}t^v\right)\left(N(0) - \frac{\omega}{\mu}\right).$$

Thus, if $N(0) \leq \frac{\omega}{\mu}$, then for $t > 0$, $N(t) \leq \frac{\omega}{\mu}$. Consequently, the closed set Υ is positively invariant with respect to fractional model (1). □

3.2 Equilibrium points

To determine the equilibrium points of fractional-order system (1), we solve the following equations:

$$^{C}D^v S(t) = {}^{C}D^v E(t) = {}^{C}D^v I(t) = {}^{C}D^v R(t) = 0.$$

By solving the algebraic equations, we obtain equilibrium points of system (1). The disease-free equilibrium point is obtained as $E_0 = (\frac{\omega}{\mu}, 0, 0, 0, 0, 0)$. In addition, if $R_0 > 1$, then system (1) has a positive endemic equilibrium point $E_1 = (S^*, E^*, I^*, R^*)$, so that

$$S^* = \frac{(\lambda + \mu)(\tau + \mu + \delta)}{\beta_1(\tau + \mu + \delta) + \beta_2\lambda},$$
$$E^* = \frac{\beta_1\omega(\tau + \mu + \delta) + \beta_2\lambda\omega - \mu(\lambda + \mu)(\tau + \mu + \delta)}{(\lambda + \mu)(\beta_1(\tau + \mu + \delta) + \beta_2\lambda)},$$
$$I^* = \frac{\lambda(\beta_1\omega(\tau + \mu + \delta) + \beta_2\lambda\omega - \mu(\lambda + \mu)(\tau + \mu + \delta))}{(\lambda + \mu)(\beta_1(\tau + \mu + \delta) + \beta_2\lambda)(\tau + \mu + \delta)},$$
$$R^* = \frac{\tau\lambda(\beta_1\omega(\tau + \mu + \delta) + \beta_2\lambda\omega - \mu(\lambda + \mu)(\tau + \mu + \delta))}{(\lambda + \mu)(\beta_1(\tau + \mu + \delta) + \beta_2\lambda)(\tau + \mu + \delta)\mu}.$$

Also, R_0 is the basic reproduction number and is obtained using the next generation method [43]. To find R_0, we first consider the system as follows:

$$^{C}D^v\Psi(t) = F\left(\Psi(t)\right) - V\left(\Psi(t)\right),$$

where

$$F\big(\Psi(t)\big) = \theta^{1-\nu} \begin{bmatrix} (\beta_1 E(t) + \beta_2 I(t))S(t) \\ 0 \end{bmatrix}$$

and

$$V\big(\Psi(t)\big) = \theta^{1-\nu} \begin{bmatrix} (\lambda + \mu)E(t) \\ -\lambda E(t) + (\tau + \mu + \delta)I(t) \end{bmatrix}.$$

At E^0, the Jacobian matrix for F and V is obtained as follows:

$$J_F(E_0) = \theta^{1-\nu} \begin{bmatrix} \beta_1 \frac{\omega}{\mu} & \beta_2 \frac{\omega}{\mu} \\ 0 & 0 \end{bmatrix}, \qquad J_\nu(E_0) = \theta^{1-\nu} \begin{bmatrix} \lambda + \mu & 0 \\ -\lambda & \tau + \mu + \delta \end{bmatrix}.$$

FV^{-1} is the next generation matrix for system (1) and the basic reproduction number is obtained from $R_0 = \rho(FV^{-1})$, so we get

$$R_0 = \frac{\beta_1 \omega(\tau + \mu + \delta) + \beta_2 \omega\lambda}{\mu(\lambda + \mu)(\tau + \mu + \delta)}.$$

This basic reproduction number R_0 is an epidemiologic metric used to describe the contagiousness or transmissibility of infectious agents.

3.3 R_0 sensitivity analysis

To check the R_0 sensitivity, we calculate its derivatives as follows:

$$\frac{\partial R_0}{\partial \beta_1} = \frac{\omega}{\mu(\lambda + \mu)},$$

$$\frac{\partial R_0}{\partial \beta_2} = \frac{\omega\lambda}{\mu(\lambda + \mu)(\tau + \mu + \delta)},$$

$$\frac{\partial R_0}{\partial \omega} = \frac{\beta_1(\tau + \mu + \delta) + \beta_2\lambda}{\mu(\lambda + \mu)(\tau + \mu + \delta)},$$

$$\frac{\partial R_0}{\partial \lambda} = \frac{\beta_2\omega(2\lambda + \mu) - \beta_1\omega(\tau + \mu + \delta)}{\mu(\lambda + \mu)^2(\tau + \mu + \delta)},$$

$$\frac{\partial R_0}{\partial \tau} = \frac{\beta_1\omega(\tau + \mu + \delta)^2 - \beta_1\omega(\tau + \mu + \delta) + \beta_2\omega\lambda}{\mu(\lambda + \mu)(\tau + \mu + \delta)^2},$$

$$\frac{\partial R_0}{\partial \delta} = \frac{\beta_1\omega(\tau + \mu + \delta)^2 - \beta_1\omega(\tau + \mu + \delta) + \beta_2\omega\lambda}{\mu(\lambda + \mu)(\tau + \mu + \delta)^2},$$

$$\frac{\partial R_0}{\partial \mu} = \frac{\beta_1\omega\mu - \beta_1\omega(\tau + \mu + \delta) - \beta_2\omega\lambda}{\mu^2(\lambda + \mu)(\tau + \mu + \delta)}$$

$$- \frac{\beta_1\omega(\tau + \mu + \delta) + \beta_2\omega\lambda}{\mu(\lambda + \mu)^2(\tau + \mu + \delta)} - \frac{\beta_1\omega(\tau + \mu + \delta) + \beta_2\omega\lambda}{\mu(\lambda + \mu)(\tau + \mu + \delta)^2}.$$

Because all the parameters are positive, so $\frac{\partial R_0}{\partial \beta_1} > 0$, $\frac{\partial R_0}{\partial \beta_2} > 0$, $\frac{\partial R_0}{\partial \omega} > 0$. Thus R_0 is increasing with β_1, β_2, ω, but we cannot say anything about other parameters here.

4 Stability of equilibrium points

In this section we investigate the stability of equilibrium points. The Jacobian matrix of system (1) is obtained as follows:

$$
J = \theta^{1-\nu}
\begin{bmatrix}
-(\beta_1 E + \beta_2 I) - \mu & -\beta_1 S & -\beta_2 S & 0 \\
\beta_1 E + \beta_2 I & \beta_1 S - (\lambda + \mu) & \beta_2 S & 0 \\
0 & \lambda & -(\tau + \mu + \delta) & 0 \\
0 & 0 & \tau & -\mu
\end{bmatrix}.
$$

So, the Jacobian matrix of system at E_0 is

$$
J(E_0) = \theta^{1-\nu}
\begin{bmatrix}
-\mu & -\beta_1 \frac{\omega}{\mu} & -\beta_2 \frac{\omega}{\mu} & 0 \\
0 & \beta_1 \frac{\omega}{\mu} - (\lambda + \mu) & \beta_2 \frac{\omega}{\mu} & 0 \\
0 & \lambda & -(\tau + \mu + \delta) & 0 \\
0 & 0 & \tau & -\mu
\end{bmatrix}.
$$

Theorem 6 *The equilibrium point E_0 of system (1) is locally asymptotically stable if $R_0 < 1$ and E_0 is unstable if $R_0 > 1$.*

Proof The characteristic equation of the Jacobian matrix at the disease-free equilibrium point $J(E_0)$ is $det(J(E_0) - kI) = 0$. Then we obtain

$$
-\theta^{1-\nu}(k + \mu)^2 \left(k^2 + Ak + B\right) = 0,
$$

where $A = -\frac{\beta_1 \omega - \mu(\lambda + \mu) - \mu(\tau + \mu + \delta)}{\mu}$ and $B = -\frac{\beta_1 \omega(\tau + \mu + \delta) - \mu(\lambda + \mu)(\tau + \mu + \delta) + \lambda \beta_2 \omega}{\mu}$. The eigenvalues of the characteristic equation are $k = -\mu$ and the roots of the equation

$$
k^2 + Ak + B = 0.
$$

If $R_0 < 1$, since all of the parameters are positive, then

$$
\beta_1 \omega(\tau + \mu + \delta) + \beta_2 \omega \lambda < \mu(\lambda + \mu)(\tau + \mu + \delta),
$$

$$
\frac{\beta_1 \omega(\tau + \mu + \delta) + \beta_2 \omega \lambda - \mu(\lambda + \mu)(\tau + \mu + \delta)}{\mu} < 0 \quad \Rightarrow \quad A > 0.
$$

Also, from $R_0 < 1$ we have

$$
\beta_1 \omega - \mu(\lambda + \mu) < \frac{-\beta_2 \omega \lambda}{\tau + \mu + \delta} < 0 \quad \Rightarrow \quad \frac{\beta_1 \omega - \mu(\lambda + \mu) - \mu(\tau + \mu + \delta)}{\mu} < 0
$$

$$
\Rightarrow \quad B > 0.
$$

Applying the Routh–Hurwitz criterion, E_0 is locally asymptotically stable. If $R_0 > 1$, then $B < 0$, and there is one positive real root for Eq.(ref2), then E_0 will be unstable.   □

The Jacobian matrix of system (1) at the endemic equilibrium point is

$$J(E_1) = \theta^{1-\nu} \begin{bmatrix} -(\beta_1 E^* + \beta_2 I^*) - \mu & -\beta_1 S^* & -\beta_2 S^* & 0 \\ \beta_1 E^* + \beta_2 I^* & \beta_1 S^* - (\lambda + \mu) & \beta_2 S^* & 0 \\ 0 & \lambda & -(\tau + \mu + \delta) & 0 \\ 0 & 0 & \tau & -\mu \end{bmatrix}.$$

The characteristic equation of matrix $J(E_1)$ is obtained as follows:

$$\theta^{1-\nu}(k + \mu)\big(k + (\mu + \delta + \tau)\big)\big(k^2 - A_1 k + B_1\big) = 0,$$

where

$$A_1 = \beta_1 S^* - \lambda - 2\mu + \frac{\beta_2 S^* \lambda}{\mu + \tau + \delta},$$

$$B_1 = \big(\mu + \beta_1 E^* + \beta_2 I^*\big)(\lambda + \mu) + \left(\frac{(\beta_1 S^* - \lambda - \mu)(\mu + \tau + \delta) + \beta_2 S^* \lambda}{\mu + \tau + \delta} \right).$$

The eigenvalues of the characteristic equation are $k_1 = -\mu$, $k_2 = -(\mu + \delta + \tau)$ and the roots of the equation

$$k^2 - A_1 k + B_1 = 0. \tag{2}$$

Since k_1, k_2 are negative, so E_1 is locally asymptotically stable when two roots of Eq. (2) are negative, so it is enough to have $B_1 > 0$ and $A_1 < 0$.

5 Existence and uniqueness of solution

In this section we show that the system has a unique solution. First, we write system (1) as follows:

$$\begin{cases} \theta^{\nu-1\,C} D_t^\nu S(t) = Q_1(t, S(t)), \\ \theta^{\nu-1\,C} D_t^\nu E(t) = Q_2(t, E(t)), \\ \theta^{\nu-1\,C} D_t^\nu I(t) = Q_3(t, I(t)), \\ \theta^{\nu-1\,C} D_t^\nu R(t) = Q_4(t, R(t)). \end{cases}$$

By taking integral form on both sides of the above equations, we get

$$\begin{cases} S(t) - S(0) = \frac{\theta^{1-\nu}}{\Gamma(\nu)} \int_0^t Q_1(\tau, S)(t - \tau)^{\nu-1}\, d\tau, \\ E(t) - E(0) = \frac{\theta^{1-\nu}}{\Gamma(\nu)} \int_0^t Q_2(\tau, E)(t - \tau)^{\nu-1}\, d\tau, \\ I(t) - I(0) = \frac{\theta^{1-\nu}}{\Gamma(\nu)} \int_0^t Q_3(\tau, I)(t - \tau)^{\nu-1}\, d\tau, \\ A(t) - A(0) = \frac{\theta^{1-\nu}}{\Gamma(\nu)} \int_0^t Q_4(\tau, A)(t - \tau)^{\nu-1}\, d\tau. \end{cases} \tag{3}$$

We show that the kernels $Q_i, i = 1, 2, 3, 4$, satisfy the Lipschitz condition and contraction.

Theorem 7 *The kernel Q_1 satisfies the Lipschitz condition and contraction if the following inequality holds:*

$$0 \leq \beta_1 d_2 + \beta_2 d_3 + \mu < 1.$$

Proof For S and S_1 we have

$$\|Q_1(t,S) - Q_1(t,S_1)\| = \|-(\beta_1 E(t) + \beta_2 I(t))(S(t) - S_1(t)) - \mu(S(t) - S_1(t))\|$$

$$\leq \|\beta_1 E(t) + \beta_2 I(t)\| \|S(t) - S_1(t)\| + \mu \|S(t) - S_1(t)\|$$

$$\leq (\beta_1 \|E(t)\| + \beta_2 \|I(t)\|) + \mu) \|S(t) - S_1(t)\|$$

$$\leq (\beta_1 d_2 + \beta_2 d_3 + \mu) \|S(t) - S_1(t)\|.$$

Suppose that $h_1 = \beta_1 d_2 + \beta_2 d_3 + \mu$, where $\|E(t)\| \leq d_2$, $\|I(t)\| \leq d_3$ are bounded functions. So

$$\|Q_1(t,S) - Q_1(t,S_1)\| \leq h_1 \|(S(t) - S_1(t))\|. \tag{4}$$

Thus, for Q_1 the Lipschitz condition is obtained, and if $0 \leq \beta_1 d_2 + \beta_2 d_3 + \mu < 1$, then Q_1 is a contraction. □

In the same way, we can prove that Q_j, $j = 2, 3, 4$, satisfy the Lipschitz condition as follows:

$$\begin{cases} \|Q_2(t,E) - Q_2(t,E_1)\| \leq h_2 \|(E(t) - E_1(t))\|, \\ \|Q_3(t,I) - Q_3(t,I_1)\| \leq h_3 \|(I(t) - I_1(t))\|, \\ \|Q_4(t,R) - Q_4(t,R_1)\| \leq h_4 \|(R(t) - R_1(t))\|, \end{cases}$$

where $\|S(t)\| \leq d_1$, and $h_2 = \beta_1 d_1 + \lambda + \mu$, $h_3 = \tau + \mu + \delta$, $h_4 = \mu$ are bounded functions. If for $j = 2, 3, 4$ we have $0 \leq h_j < 1$, then Q_j are contractions for $j = 2, 3, 4$. According to system (3), consider the following recursive forms:

$$\psi_{1n}(t) = S_n(t) - S_{n-1}(t) = \frac{\theta^{1-\nu}}{\Gamma(\nu)} \int_0^t (Q_1(\tau, S_{n-1}) - Q_1(\tau, S_{n-2}))(t-\tau)^{\nu-1} d\tau,$$

$$\psi_{2n}(t) = E_n(t) - E_{n-1}(t) = \frac{\theta^{1-\nu}}{\Gamma(\nu)} \int_0^t (Q_2(\tau, E_{n-1}) - Q_2(\tau, E_{n-2}))(t-\tau)^{\nu-1} d\tau,$$

$$\psi_{3n}(t) = I_n(t) - I_{n-1}(t) = \frac{\theta^{1-\nu}}{\Gamma(\nu)} \int_0^t (Q_3(\tau, I_{n-1}) - Q_3(\tau, I_{n-2}))(t-\tau)^{\nu-1} d\tau,$$

$$\psi_{4n}(t) = R_n(t) - R_{n-1}(t) = \frac{\theta^{1-\nu}}{\Gamma(\nu)} \int_0^t (Q_4(\tau, R_{n-1}) - Q_4(\tau, R_{n-2}))(t-\tau)^{\nu-1} d\tau,$$

with the initial conditions $S_0(t) = S(0)$, $E_0(t) = E(0)$, $I_0(t) = I(0)$, and $R_0(t) = R(0)$. We take the norm of the first equation in the above system, then

$$\|\psi_{1n}(t)\| = \|S_n(t) - S_{n-1}(t)\|$$

$$= \left\| \frac{\theta^{1-\nu}}{\Gamma(\nu)} \int_0^t (Q_1(\tau, S_{n-1}) - Q_1(\tau, S_{n-2}))(t-\tau)^{\nu-1} d\tau \right\|$$

$$\leq \frac{\theta^{1-\nu}}{\Gamma(\nu)} \int_0^t \|Q_1(\tau, S_{n-1}) - Q_1(\tau, S_{n-2}))(t-\tau)^{\nu-1}\| d\tau,$$

with Lipschitz condition (4), we have

$$\left\| \psi_{1n}(t) \right\| \leq \frac{\theta^{1-\nu}}{\Gamma(\nu)} h_1 \int_0^t \left\| \psi_{1(n-1)}(\tau) \right\| d\tau. \tag{5}$$

In a similar way, we obtain

$$\left\| \psi_{2n}(t) \right\| \leq \frac{\theta^{1-\nu}}{\Gamma(\nu)} h_2 \int_0^t \left\| \psi_{2(n-1)}(\tau) \right\| d\tau,$$

$$\left\| \psi_{3n}(t) \right\| \leq \frac{\theta^{1-\nu}}{\Gamma(\nu)} h_3 \int_0^t \left\| \psi_{3(n-1)}(\tau) \right\| d\tau,$$

$$\left\| \psi_{4n}(t) \right\| \leq \frac{\theta^{1-\nu}}{\Gamma(\nu)} h_4 \int_0^t \left\| \psi_{4(n-1)}(\tau) \right\| d\tau. \tag{6}$$

Thus, we can write that

$$S_n(t) = \sum_{i=1}^n \psi_{1i}(t), E_n(t) = \sum_{i=1}^n \psi_{2i}(t), I_n(t) = \sum_{i=1}^n \psi_{3i}(t), R_n(t) = \sum_{i=1}^n \psi_{4i}(t).$$

In the next theorem, we prove the existence of a solution.

Theorem 8 *A system of solutions given by the fractional COVID-19 SEIR model* (1) *exists if there exists t_1 such that*

$$\frac{\theta^{1-\nu}}{\Gamma(\nu)} t_1 h_j < 1.$$

Proof From the recursive technique and Eq. (5) and Eq. (6) we conclude that

$$\left\| \psi_{1n}(t) \right\| \leq \left\| S_n(0) \right\| \left[\frac{\theta^{1-\nu}}{\Gamma(\nu)} h_1 t \right]^n,$$

$$\left\| \psi_{2n}(t) \right\| \leq \left\| E_n(0) \right\| \left[\frac{\theta^{1-\nu}}{\Gamma(\nu)} h_2 t \right]^n,$$

$$\left\| \psi_{3n}(t) \right\| \leq \left\| I_n(0) \right\| \left[\frac{\theta^{1-\nu}}{\Gamma(\nu)} h_3 t \right]^n,$$

$$\left\| \psi_{4n}(t) \right\| \leq \left\| R_n(0) \right\| \left[\frac{\theta^{1-\nu}}{\Gamma(\nu)} h_4 t \right]^n.$$

Thus, the system has a solution and also it is continuous. Now we show that the above functions construct solution for model (3). We assume that

$$S(t) - S(0) = S_n(t) - B_{1n}(t),$$

$$E(t) - E(0) = E_n(t) - B_{2n}(t),$$

$$I(t) - I(0) = I_n(t) - B_{3n}(t),$$

$$R(t) - R(0) = R_n(t) - B_{4n}(t).$$

So

$$\left\| B_{1n}(t) \right\| = \left\| \frac{\theta^{1-\nu}}{\Gamma(\nu)} \int_0^t \left(Q_1(\tau, S) - Q_1(\tau, S_{n-1}) \right) d\tau \right\|$$

$$\leq \frac{\theta^{1-\nu}}{\Gamma(\nu)} \int_0^t \left\| Q_1(\tau, S) - Q_1(\tau, S_{n-1}) \right\| d\tau$$

$$\leq \frac{\theta^{1-\nu}}{\Gamma(\nu)} h_1 \| S - S_{n-1} \| t.$$

By repeating the method, we obtain

$$\left\| B_{1n}(t) \right\| \leq \left[\frac{\theta^{1-\nu}}{\Gamma(\nu)} t \right]^{n+1} h_1^{n+1} k.$$

At t_1, we get

$$\left\| B_{1n}(t) \right\| \leq \left[\frac{\theta^{1-\nu}}{\Gamma(\nu)} t_1 \right]^{n+1} h_1^{n+1} k.$$

Taking limit on the recent equation as n approaches ∞, we obtain $\| B_{1n}(t) \| \to 0$. In the same way, we can show that $\| B_{jn}(t) \| \to 0$, $j = 2, 3, 4$. This completes the proof. □

To show the uniqueness of the solution, we suppose that the system has another solution such as $S_1(t)$, $E_1(t)$, $I_1(t)$, and $R_1(t)$, then we have

$$S(t) - S_1(t) = \frac{\theta^{1-\nu}}{\Gamma(\nu)} \int_0^t \left(Q_1(\tau, S) - Q_1(\tau, S_1) \right) d\tau.$$

We take norm from this equation

$$\left\| S(t) - S_1(t) \right\| = \frac{\theta^{1-\nu}}{\Gamma(\nu)} \int_0^t \left\| Q_1(\tau, S) - Q_1(\tau, S_1) \right\| d\tau.$$

It follows from Lipschitz condition (4) that

$$\left\| S(t) - S_1(t) \right\| \leq \frac{\theta^{1-\nu}}{\Gamma(\nu)} h_1 t \left\| S(t) - S_1(t) \right\|.$$

Thus

$$\left\| S(t) - S_1(t) \right\| \left(1 - \frac{\theta^{1-\nu}}{\Gamma(\nu)} h_1 t \right) \leq 0. \tag{7}$$

Theorem 9 *The solution of COVID-19 SEIR model* (1) *is unique if the following condition holds*:

$$1 - \frac{\theta^{1-\nu}}{\Gamma(\nu)} h_1 t > 0.$$

Proof Suppose that condition (7) holds

$$\|S(t) - S_1(t)\| \left(1 - \frac{\theta^{1-\nu}}{\Gamma(\nu)} h_1 t \right) \le 0.$$

Then $\|S(t) - S_1(t)\| = 0$. So, we obtain $S(t) = S_1(t)$. Similarly, we can show the same equality for E, I, R. □

6 Numerical results

Using the fractional Euler method for Caputo derivative, we present approximate solutions for the fractional-order COVID-19 SEIR model [44]. We present simulations to predict the COVID-19 transmission in the world.

6.1 Numerical method

We consider system (1) in a compact form as follows:

$$\theta^{\nu-1\,C}D_t^\nu w(t) = g(t, w(t)), \quad w(0) = w_0, 0 \le t \le T < \infty, \tag{8}$$

where $w = (S, E, I, R) \in R_+^4$, $w_0 = (S_0, E_0, I_0, R_0)$ is the initial vector, and $g(t) \in R$ is a continuous vector function satisfying Lipschitz condition

$$\|g(w_1(t)) - g(w_2(t))\| \le k \|w_1(t) - w_2(t)\|, \quad k > 0.$$

Applying a fractional integral operator corresponding to the Caputo derivative to equation (8), we obtain

$$w(t) = \theta^{1-\nu} [w_0 + I^\nu g(w(t))], \quad 0 \le t \le T < \infty.$$

Set $h = \frac{T-0}{N}$ and $t_n = nh$, where $t \in [0, T]$ and N is a natural number and $n = 0, 1, 2, \ldots, N$. Let w_n be the approximation of $w(t)$ at $t = t_n$. Using the fractional Euler method [44], we get

$$w_{n+1} = \theta^{1-\nu} \left[w_0 + \frac{h^\nu}{\Gamma(\nu+1)} \sum_{j=0}^n u_{n+1,j} g(t_j, w_j) \right], \quad j = 0, 1, 2, \ldots, N-1,$$

where

$$u_{n+1,j} = (n+1-j)^\nu - (n-j)^\nu, \quad j = 0, 1, 2, \ldots, n.$$

The stability analysis of the obtained scheme has been proved in Theorem (3.1) in [44].

Thus, the solution of system (1) is written as follows:

$$S_{n+1} = \theta^{1-\nu} \left[S_0 + \frac{h^\nu}{\Gamma(\nu+1)} \sum_{j=0}^n u_{n+1,j} f_1(t_j, w_j) \right],$$

$$E_{n+1} = \theta^{1-\nu} \left[E_0 + \frac{h^\nu}{\Gamma(\nu+1)} \sum_{j=0}^n u_{n+1,j} f_2(t_j, w_j) \right],$$

$$I_{n+1} = \theta^{1-\nu}\left[I_0 + \frac{h^\nu}{\Gamma(\nu+1)}\sum_{j=0}^{n} u_{n+1,j}f_3(t_j, w_j)\right],$$

$$R_{n+1} = \theta^{1-\nu}\left[R_0 + \frac{h^\nu}{\Gamma(\nu+1)}\sum_{j=0}^{n} u_{n+1,j}f_4(t_j, w_j)\right],$$

where $u_{n+1,j} = (n+1-j)^\nu - (n-i)^\nu$, $f_1(t, w(t)) = \omega - (\beta_1 E(t) + \beta_2 I(t))S(t) - \mu S(t)$, $f_2(t, w(t)) = (\beta_1 E(t) + \beta_2 I(t))S(t) - (\lambda + \mu)E(t)$, $f_3(t, w(t)) = \lambda E(t) - (\tau + \mu + \delta)I(t)$, $f_4(t, w(t)) = \tau I(t) - \mu R(t)$.

6.2 Simulation

Case I: The world

To provide a numerical simulation, we must first determine the value of the parameters. The current birth rate for the world in 2020 is 18.077 births per 1000 people, and the death rate is 7.612 per 1000 people [45]. The world's population on 4 February was $N = 7610105452$, so $\omega = \frac{n \times N}{365} = 391347.066$ and $\mu = \frac{7.612}{365 \times 1000} = 2.08547 \times 10^{-5}$, and we choose $\theta = 0.99$. Since $N(0) = S(0) + E(0) + I(0) + R(0)$ and on 4 February we have $I(0) = 24545$, $R(0) = 907$ [46], then we assume $E(0) = 80000$ and $S(0) = 7610026000$. Also, according to the WHO report, the COVID-19 mortality rate is $\delta = 3.4 \times 10^{-2}$ [46]. To estimate other parameters, we use the fitting curve technique with the real data reported for COVID-19. The fitted curve and the reported cumulative number of COVID-19 in the world from 4 February to 12 May 2020 are plotted in Fig. 2, so that every part is a week. Using this method, we obtain the parameters as follows: $\beta_1 = 2 \times 10^{-11}$, $\beta_2 = 2.2 \times 10^{-9}$, $\lambda = 2.35 \times 10^{-5}$, $\tau = 0.03$.

Table 1 compares the absolute and relative errors for I(t) concerning the fractional- and integer-order models with respect to the reported cases of infected people. From this table, you can observe that the Caputo model with $\nu = 0.97$ provides more realistic results than the classic model with integer-order derivatives.
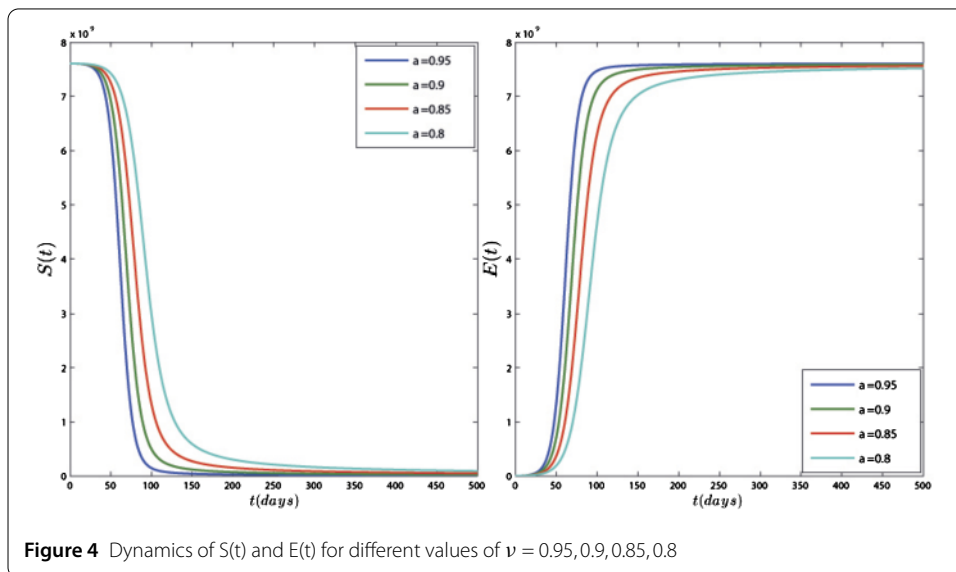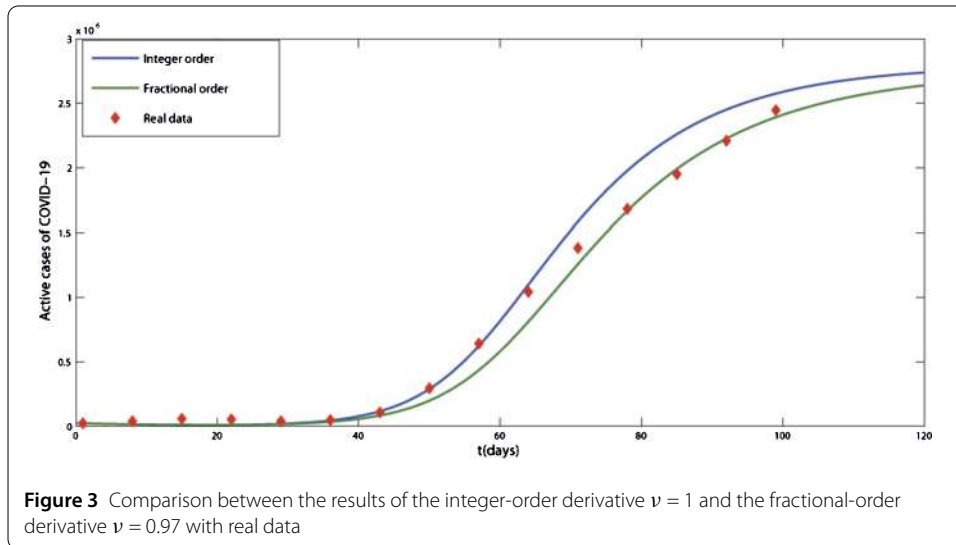
A comparison between the noninteger-order model with $\nu = 0.97$ and the integer-order one with $\nu = 1$ and the real data for the infected cases of the COVID-19 from 4 February to
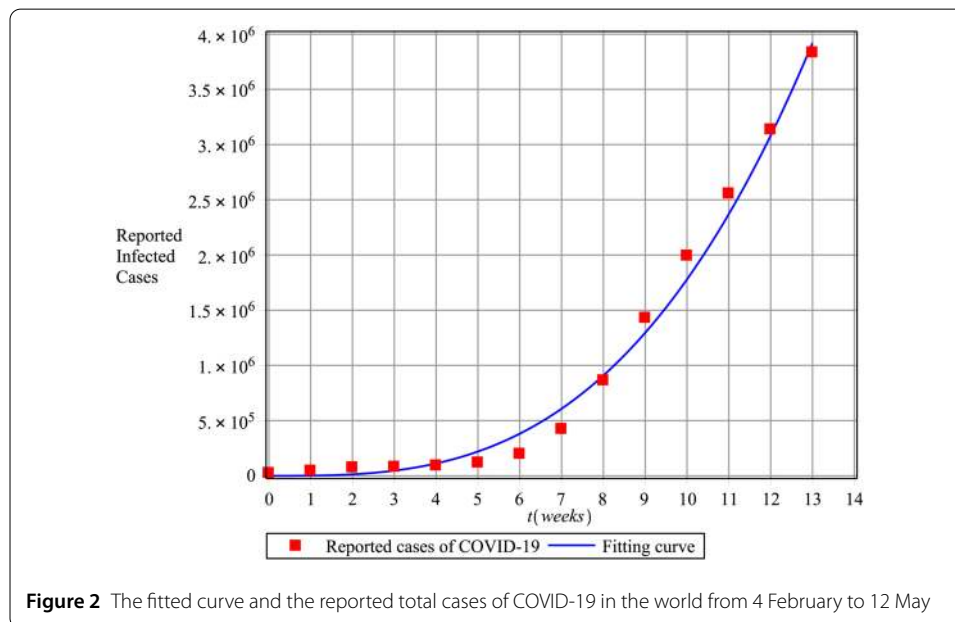
Figure 2 The fitted curve and the reported total cases of COVID-19 in the world from 4 February to 12 May

Table 1 The absolute and relative errors for *I*(*t*)

Model	ν	Absolute error	Relative error
Fractional	0.97	7.23451	0.0312
Integer	–	9.04562	0.0394

Figure 3 Comparison between the results of the integer-order derivative $\nu = 1$ and the fractional-order derivative $\nu = 0.97$ with real data

Figure 4 Dynamics of S(t) and E(t) for different values of $\nu = 0.95, 0.9, 0.85, 0.8$

12 May is also given in Fig. 3. The obtained results show that the answer of the fractional-order model corresponds well with the real data and together with the results of Table 1 shows the advantage of using the fractional-order derivative instead of the correct order one.

In Figs. 4 and 5, we have plotted the results of model (1) for different values of ν. In this simulation, the equilibrium point is

$$E_1 = \left(S^*, E^*, I^*, R^*\right) = \left(2.5 \times 10^6, 7.52 \times 10^9, 2.76 \times 10^6, 2.9 \times 10^9\right).$$
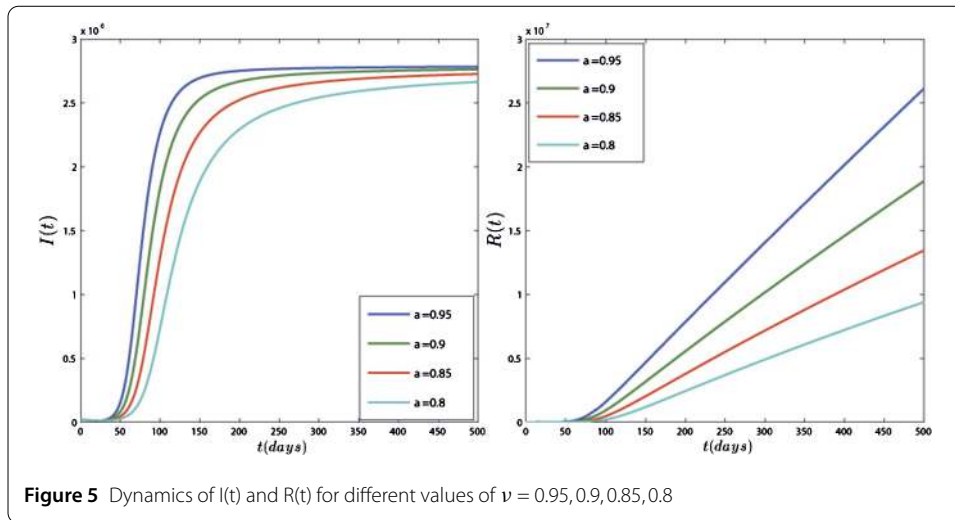
Figure 5 Dynamics of I(t) and R(t) for different values of $\nu = 0.95, 0.9, 0.85, 0.8$
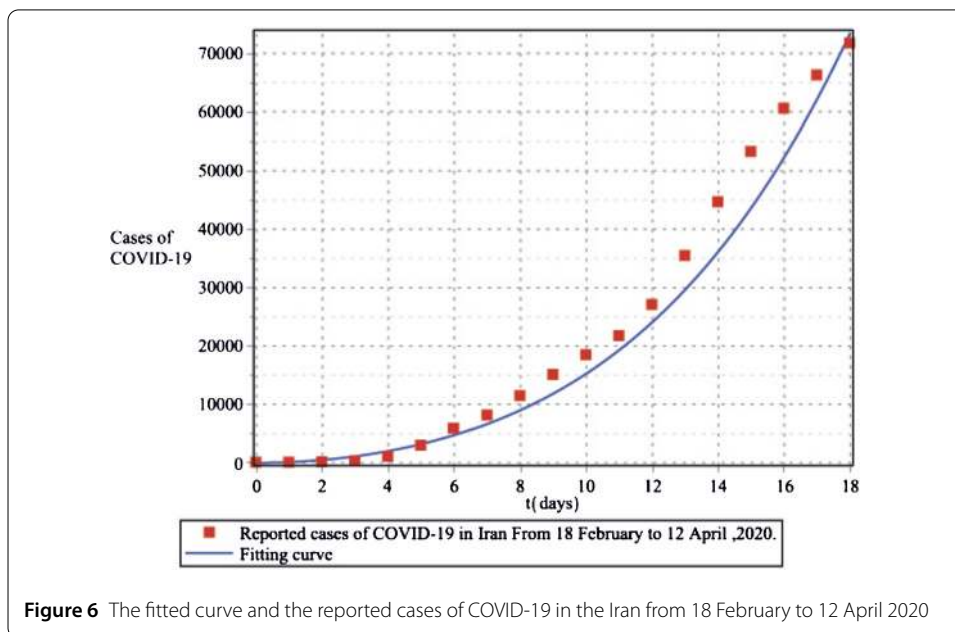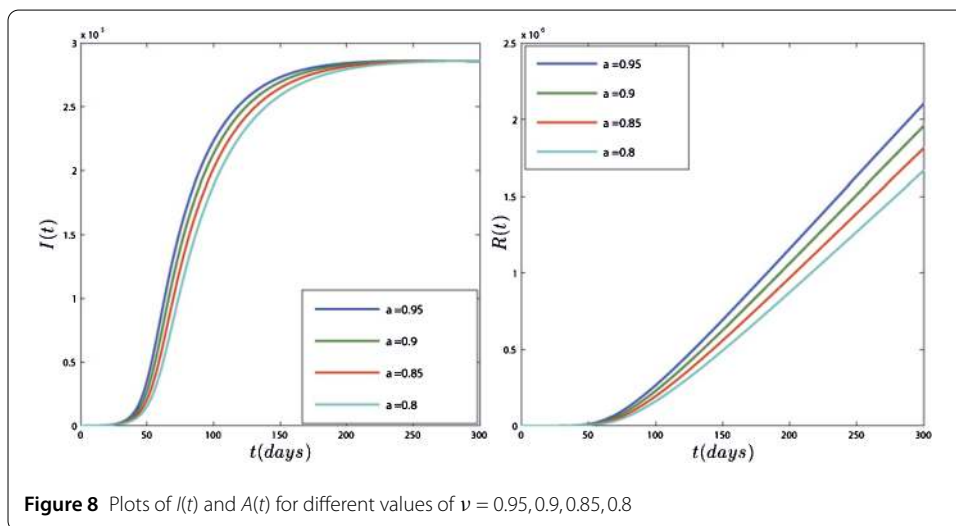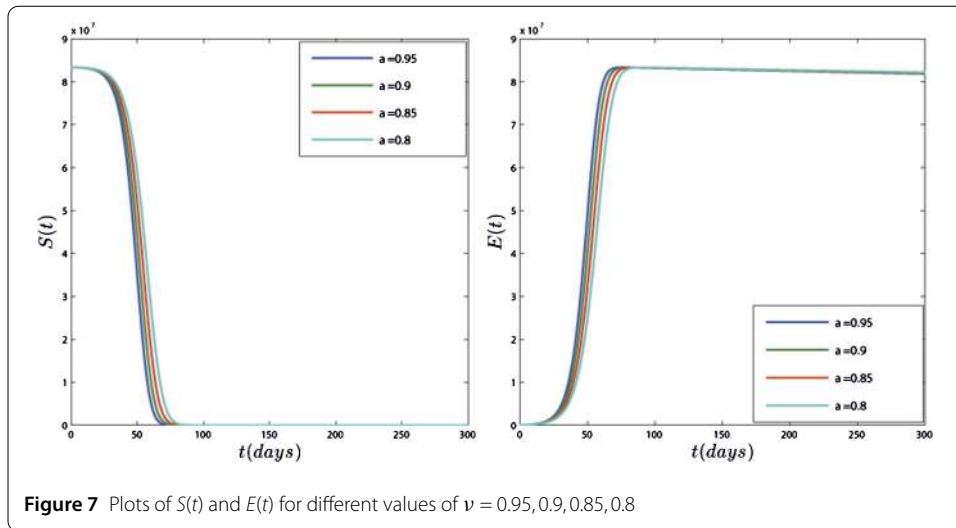

Figure 6 The fitted curve and the reported cases of COVID-19 in the Iran from 18 February to 12 April 2020

Figures 4 and 5 show that the results of the model converge to their equilibrium point for different orders of derivation, and the results of all orders are stable at the equilibrium points. These figures show that the obtained plots for different values of ν are different in quantity but they have the same behavior. Also, Fig. 5 shows that approximately 50 days after 4 February 2020 the number of active cases ceases to increase and becomes stable in 2.76×10^6.

Case II: Iran

In the second case, we provide a numerical simulation using real data for the transmission model of COVID-19 in Iran. According to the WHO report, the total population of Iran on 18 February 2020 was $N = 83392425$, the birth rate for Iran in 2019 was 18.547 births per 1000 people, and the death rate was 4.866 per 1000 people. Thus, for every day, we have $\omega = \frac{n \times N}{365} = 4237.477$ and $\mu = \frac{0.004866}{365} = 0.0000133315$. Similarly, we assumed the mortality rate due to the disease in Iran is $\delta = 3.4 \times 10^{-2}$ and $\theta = 0.99$. Since

Figure 7 Plots of $S(t)$ and $E(t)$ for different values of $\nu = 0.95, 0.9, 0.85, 0.8$

Figure 8 Plots of $I(t)$ and $A(t)$ for different values of $\nu = 0.95, 0.9, 0.85, 0.8$

$N(0) = S(0) + E(0) + I(0) + R(0)$ and on 18 February we have $I(0) = 61$, $R(0) = 12$, then we assume $E(0) = 3000$ and $S(0) = 83{,}389{,}352$. For the fitting, we use the information provided by the World Health Organization for COVID-19. The fitted curve and the reported cases of COVID-19 in Iran from 18 February to 12 April 2020 are plotted in Fig. 6, so that every part is three days. Using this method, we obtain the parameters as follows: $\beta_1 = 1.1 \times 10^{-4}$, $\beta_2 = 3.3 \times 10^{-6}$, $\lambda = 1.02 \times 10^{-3}$, $\tau = 0.03$. In Figs. 7 and 8, we plotted the results of the system of COVID-19 transmission (1). As you can see in Figs. 7 and 8, the variables have different results in different amounts of ν but exhibit the same behavior. Figure 7 shows that two months after the virus is released almost the entire population is at risk for the disease. Figure 8 shows that the number of people with COVID-19 increases until 200 days and then stabilizes. Also, the forecast is that the number of infected people could rise to 280,000. Also, Fig. 8 shows that the number of people who have recovered or died also increases over time.

7 Conclusion

In this work, the SEIR epidemic model for the transmission of COVID-19 using the Caputo fractional derivative has been presented. The feasibility region of the system and equilibrium points have been calculated, and the stability of the equilibrium points has been investigated. The existence of a unique solution for the model by using fixed point theory has been proved. Using the fractional Euler method, an approximate answer to the model has been calculated. To predict the transmission of COVID-19 in the world and in Iran, the numerical simulations based on real data have been provided. Also in the numerical section, we have examined the advantage of using the fractional-order derivative instead of the integer-order one, and in Table 1 and Fig. 3, we have compared the results of the model with the fractional- and integer-order derivative and the real data. The results show that the fractional-order model has a better result in this modeling.

Availability of data and materials
Data sharing not applicable to this article as no datasets were generated or analyzed during the current study.

Ethics approval and consent to participate
Not applicable.

Competing interests
The authors declare that they have no competing interests.

Consent for publication
Not applicable.

Authors' contributions
The authors declare that the study was realized in collaboration with equal responsibility. All authors read and approved the final manuscript.

Authors' information
Shahram Rezapour: shahramrezapour@duytan.edu.vn, sh.rezapour@mail.cmuh.org.tw, sh.rezapour@azaruniv.ac.ir, rezapourshahram@yaho.ca

Author details
[1]Institute of Research and Development, Duy Tan University, Da Nang 550000, Vietnam. [2]Faculty of Natural Sciences, Duy Tan University, Da Nang 550000, Vietnam. [3]Department of Medical Research, China Medical University Hospital, China Medical University, Taichung, Taiwan. [4]Department of Mathematics, Miandoab Branch, Islamic Azad University, Miandoab, Iran. [5]Department of Mathematics, Bu-Ali Sina University, 65178 Hamedan, Iran.

Publisher's Note

Springer Nature remains neutral with regard to jurisdictional claims in published maps and institutional affiliations.

References
 1. Haq, F., Shah, K., Rahman, G., Shahzad, M.: Numerical analysis of fractional order model of HIV-1 infection of CD4+ T-cells. Comput. Methods Differ. Equ. **5**(1), 1–11 (2017)
 2. Koca, I.: Analysis of rubella disease model with non-local and non-singular fractional derivatives. Int. J. Optim. Control Theor. Appl. **8**(1), 17–25 (2018)
 3. Rida, S.Z., Arafa, A.A.M., Gaber, Y.A.: Solution of the fractional epidemic model by l-adm. J. Fract. Calc. Appl. **7**(1), 189–195 (2016)
 4. Singh, H., Dhar, J., Bhatti, H.S., Chandok, S.: An epidemic model of childhood disease dynamics with maturation delay and latent period of infection. Model. Earth Syst. Environ. **2**, 79 (2016)
 5. Tchuenche, J.M., Dube, N., Bhunu, C.P., Smith, R.J., Bauch, C.T.: The impact of media coverage on the transmission dynamics of human influenza. BMC Public Health **11**, 1–5 (2011)

6. Upadhyay, R.K., Roy, P.: Spread of a disease and its effect on population dynamics in an Eco-epidemiological system. Commun. Nonlinear Sci. Numer. Simul. **19**(12), 4170–4184 (2014)

7. Baleanu, D., Mohammadi, H., Rezapour, S.: A mathematical theoretical study of a particular system of Caputo–Fabrizio fractional differential equations for the Rubella disease model. Adv. Differ. Equ. **2020**, 184 (2020). https://doi.org/10.1186/s13662-020-02614-z

8. Tuan, N.H., Mohammadi, H., Rezapour, S.: A mathematical model for COVID-19 transmission by using the Caputo fractional derivative. Chaos Solitons Fractals **140**, 110107 (2020). https://doi.org/10.1016/j.chaos.2020.110107

9. Baleanu, D., Jajarmi, A., Mohammadi, H., Rezapour, S.: A new study on the mathematical modeling of human liver with Caputo–Fabrizio fractional derivative. Chaos Solitons Fractals **134**, 7 (2020)

10. Baleanu, D., Aydogan, S.M., Mohammadi, H., Rezapour, S.: On modelling of epidemic childhood diseases with the Caputo–Fabrizio derivative by using the Laplace Adomian decomposition method. Alex. Eng. J. (2020). https://doi.org/10.1016/j.aej.2020.05.007

11. Baleanu, D., Rezapour, S., Mohammadi, H.: Some existence results on nonlinear fractional differential equations. Philos. Trans. R. Soc. Lond. A **371**, 20120144 (2013). https://doi.org/10.1098/rsta.2012.0144

12. Etemad, S., Rezapour, S., Samei, M.E.: On a fractional Caputo–Hadamard inclusion problem with sum boundary value conditions by using approximate endpoint property. Math. Model. Appl. Sci. (2020). https://doi.org/10.1002/mma.6644

13. Samei, M.E., Rezapour, S.: On a system of fractional q-differential inclusions via sum of two multi-term functions on a time scale. Bound. Value Probl. **2020**, 135 (2020). https://doi.org/10.1186/s13661-020-01433-1

14. Baleanu, D., Etemad, S., Rezapour, S.: On a fractional hybrid integro-differential equation with mixed hybrid integral boundary value conditions by using three operators. Alex. Eng. J. (2020). https://doi.org/10.1016/j.aej.2020.04.053

15. Alsaedi, A., Baleanu, D., Etemad, S., Rezapour, S.: On coupled systems of time-fractional differential problems by using a new fractional derivative. J. Funct. Spaces **2016**, Article ID 4626940 (2016). https://doi.org/10.1155/2016/4626940

16. Agarwal, R.P., Baleanu, D., Hedayati, V., Rezapour, S.: Two fractional derivative inclusion problems via integral boundary conditions. Appl. Math. Comput. **257**, 205–212 (2015). https://doi.org/10.1016/j.amc.2014.10.082

17. Hedayati, V., Rezapour, S.: The existence of solution for a k-dimensional system of fractional differential inclusions with anti-periodic boundary value problems. Filomat **30**(6), 1601–1613 (2016). https://doi.org/10.2298/FIL1606601H

18. Baleanu, D., Hedayati, V., Rezapour, S., Al-Qurashi, M.M.: On two fractional differential inclusions. SpringerPlus **5**(1), 882 (2016). https://doi.org/10.1186/s40064-016-2564-z

19. Rezapour, S., Samei, M.E.: On the existence of solutions for a multi-singular pointwise defined fractional q-integro-differential equation. Bound. Value Probl. **2020**, 38 (2020). https://doi.org/10.1186/s13661-020-01342-3

20. Baleanu, D., Agarwal, R.P., Mohammadi, H., Rezapour, S.: Some existence results for a nonlinear fractional differential equation on partially ordered Banach spaces. Bound. Value Probl. **2013**, 112 (2013)

21. Baleanu, D., Mousalou, A., Rezapour, S.: On the existence of solutions for some infinite coefficient-symmetric Caputo–Fabrizio fractional integro-differential equations. Bound. Value Probl. **2017**, 145 (2017)

22. Mahdy, A.M.S., Sweilam, N.H., Higazy, M.: Approximate solution for solving nonlinear fractional order smoking model. Alex. Eng. J. **59**(2), 739–752 (2020)

23. Mahdy, A.M.S., Higazy, M., Gepreel, K.A., El-dahdouh, A.A.A.: Optimal control and bifurcation diagram for a model nonlinear fractional sirc. Alex. Eng. J. (2020). https://doi.org/10.1016/j.aej.2020.05.028

24. Losada, J., Nieto, J.J.: Properties of the new fractional derivative without singular kernel. Prog. Fract. Differ. Appl. **1**(2), 87–92 (2015)

25. Aydogan, M.S., Baleanu, D., Mousalou, A., Rezapour, S.: On high order fractional integro-differential equations including the Caputo–Fabrizio derivative. Bound. Value Probl. **2018**, 90 (2018). https://doi.org/10.1186/s13661-018-1008-9

26. Dokuyucu, M.A., Celik, E., Bulut, H., Baskonus, H.M.: Cancer treatment model with the Caputo–Fabrizio fractional derivative. Eur. Phys. J. Plus **133**, 92 (2018)

27. Khan, M.A., Hammouch, Z., Baleanu, D.: Modeling the dynamics of hepatitis e via the Caputo–Fabrizio derivative. Math. Model. Nat. Phenom. **14**(3), 311 (2019)

28. Ullah, S., Khan, M.A., Farooq, M., Hammouch, Z., Baleanu, D.: A fractional model for the dynamics of tuberculosis infection using Caputo–Fabrizio derivative. Discrete Contin. Dyn. Syst. **13**(3), 975–993 (2020)

29. Ucar, E., Ozdemir, N., Altun, E.: Fractional order model of immune cells influenced by cancer cells. Math. Model. Nat. Phenom. **14**(3), 308 (2019)

30. Saleem, M.U., Farman, M., Ahmad, A., Haque, E.U., Ahmad, M.O.: A Caputo Fabrizio fractional order model for control of glucose in insulin therapies for diabetes. Ain Shams Eng. J. (2020). https://doi.org/10.1016/j.asej.2020.03.006

31. Dighe, A., Jombart, T., Kerkhove, M.V., Ferguson, N.: A mathematical model of the transmission of middle east respiratory syndrome corona virus in dromedary camels (camelus dromedarius). Int. J. Infect. Dis. **79**(S1), 1–150 (2019)

32. Higazy, M.: Novel fractional order SIDARTHE mathematical model of COVID-19 pandemic. Chaos Solitons Fractals **138**, 110007 (2020)

33. Chen, T., Rui, J., Wang, Q., Zhao, Z., Cui, J.A., Yin, L.: A mathematical model for simulating the transmission of Wuhan novel coronavirus. Infect. Dis. Poverty **9**, 24 (2020)

34. Baleanu, D., Mohammadi, H., Rezapour, S.: A fractional differential equation model for the COVID-19 transmission by using the Caputo–Fabrizio derivative. Adv. Differ. Equ. **2020**, 299 (2020). https://doi.org/10.1186/s13662-020-02762-2

35. Naveed, M., Rafiq, M., Raza, A., Ahmed, N., Khan, I., Nisar, K.S., Soori, A.H.: Mathematical analysis of novel Coronavirus (2019-ncov) delay ppndemic model. Comput. Mater. Continua **64**(3), 1401–1414 (2020)

36. Shaikh, A.S., Jadhav, V.S., Timol, M.G., Nisar, K.S., Khan, I.: Analysis of the covid-19 pandemic spreading in india by an epidemiological model and fractional differential operator. Preprints 2020050266 (2020). https://doi.org/10.20944/preprints202005.0266.v1

37. Zhou, Y., Ma, Z., Brauer, F.: A discrete epidemic model for SARS transmission and control in China. Math. Comput. Model. **40**(13), 1491–1506 (2004)

38. Samko, S.G., Kilbas, A.A., Marichev, O.I.: Fractional Integrals and Derivatives: Theory and Applications. Gordon & Breach, Philadelphia (1993)

39. Caputo, M., Fabrizio, M.: A new definition of fractional derivative without singular kernel. Prog. Fract. Differ. Appl. **1**(2), 73–85 (2015)

40. Atangana, A., Baleanu, D.: New fractional derivatives with nonlocal and non-singular kernel: theory and application to heat transfer model. Therm. Sci. **20**(2), 763–769 (2016)
41. Ullah, M.Z., Alzahrani, A.K., Baleanu, D.: An efficient numerical technique for a new fractional tuberculosis model with nonsingular derivative operator. J. Taibah Univ. Sci. **13**(1), 1147–1157 (2019)
42. Diethelm, K.A.: The Analysis of Fractional Differential Equations. Springer, Berlin (2010)
43. Van den Driessche, P., Watmough, J.: Reproduction numbers and sub-threshold endemic equilibria for compartmental models of disease transmission. Math. Biosci. **58**, 348–352 (2012). https://doi.org/10.1016/S0025-5564(02)00108-6
44. Li, C., Zeng, F.: The finite difference methods for fractional ordinary differential equations. Numer. Funct. Anal. Optim. **34**(2), 149–179 (2013)
45. Macrotrends: The premier research platform for long term investors. 2010–2020 Macrotrends LLC. https://www.macrotrends.net
46. Worldometer: COVID-19 coronavirus pandemic. American Library Association. https://www.worldometers.info/coronavirus